

Ni/4H-SiC Ohmic Contact Formation Using Multipulse Nanosecond Laser Annealing

M. Opprecht^{1,a*}, S. Kerdilès^{1,b}, J. Biscarrat^{1,c}, P. Godignon^{1,d}, C. Masante^{1,e},
R. Laviéville^{1,f}, N. Vaxelaire^{1,g}, P. Gergaud^{1,h}, A. Grenier^{1,i}, C. Jung^{1,j},
F. Roze^{2,k}, Z. Chehadi^{2,l}, L. Thuries^{2,m}, L. Lu^{2,n}, T. Tabata^{2,o}

¹Université Grenoble Alpes, CEA LETI, Grenoble, France

²Laser Systems & Solutions of Europe (LASSE), Gennevilliers 92230, France

^{a*}mathieu.opprecht@cea.fr, ^bsébastien.kerdilès@cea.fr, ^cjerome.biscarrat@cea.fr,

^dPhilippe.godignon@cea.fr, ^ecedric.masante@cea.fr, ^fromain.lavieville@cea.fr,

^gnicolas.vaxelaire@cea.fr, ^hpatrice.gergaud@cea.fr, ⁱadeline.grenier@cea.fr, ^jcarl.jung@cea.fr

^kfabien.roze@screen-lasse.com, ^lzeinab.chehadi@utt.fr, ^mlouis.thuries@screen-lasse.com,

ⁿlu.lu@screen-lasse.com, ^otoshiyuki.tabata@screen-lasse.com

Keywords: Ohmic contact, Ni-4HsiC, Laser Annealing, Multipulse, Contact resistance

Abstract. Nowadays, the growing worldwide electrification requires new materials for power management. SiC currently dominates the market thanks to excellent energy efficiency and broad operating capabilities. The present paper proposes an experimental study of the Ni-SiC backside ohmic contact formation using 308 nm nanosecond laser annealing (NLA). After Nickel (80 nm) sputtering over 4H-SiC wafers, various laser conditions are investigated, with energy density (ED) ranging from 2.4 to 5.4 J/cm², pulse number from 1 to 20 and chuck temperature from 25 °C (RT) to 400 °C. For all series, a common scenario is noticed as the ED increases, with first solid-state reactions, then local melt and, finally, complete top layer melt and de-wetting at high ED. An in-depth understanding of the impact of laser conditions on these stages is achieved, based on electrical data, Raman spectroscopy, optical microscopy, Scanning Electron Microscopy (SEM) and Scanning Transmission Electron Microscopy (STEM). Results reveal that both high pulse numbers and the use of a hot chuck enable to significantly reduce the ED needed to form low resistance contacts. In addition, sheet resistances and contact resistivities are linked to the microstructure evolution upon NLA exposure. As a proof-of-concept, an acceptable process point yields a contact resistivity around 5×10⁻⁵ Ω cm² when the wafer is processed at 25 °C and a value as low as 10⁻⁵ Ω cm² for 400 °C processing. The mechanisms involved and discussed in the present work may very likely pave the way for other contact formation with limited thermal budget.

Introduction & Experimental Protocol

Silicon carbide (4H-SiC) is one of the best candidates to comply with power device specifications associated with sustainable development and energy issues. Recently, pulsed nanosecond laser annealing (NLA) studies showed promising results to produce back side ohmic contacts without detrimental impact on front side devices [1-3]. Most of the works focused on single laser pulses (e.g. one pulse per location). In order to provide a complete picture, both single pulse and multi-pulse (3, 5, 10 and 20 pulses) regimes are investigated in the present study over a wide range of laser energy densities (ED). Additionally, wafers are processed on a chuck at RT and 400°C. We study the behaviour of 80 nm thick Nickel (Ni) layers deposited on the C-face of 4H-SiC substrates (6×10¹⁸ cm⁻³ nitrogen doping) upon NLA. Blanket and patterned c-TLM (Circular Transfer Length Method) structures wafers are irradiated using the SCREEN_LT-3100 tool, equipped with a XeCl excimer laser (308 nm wavelength and ~160 ns Full Width at Half Maximum pulse duration). Ohmic contact electrical behaviour is evaluated thanks to the patterned c-TLM structures. In parallel, sheet resistance (R_s) and Raman spectroscopy measurements, combined with scanning (SEM) and transmission electron microscopy (TEM) observations on blanket samples enable us to correlate electrical results to microstructural evolutions.

Results & Discussions

Microstructure regimes. When varying the laser ED, three regimes are encountered for Ni-SiC samples submitted to NLA at RT. Fig.1 shows the evolution of R_s as a function of ED for various numbers of pulses. The first regime, observed at low ED, corresponds to solid-state reactions at the Ni-SiC interface. As confirmed by optical microscopy (OM) observations (Fig.1a), the top surface morphology remains unchanged compared to that of the reference (e.g. the as-deposited state). Whatever the number of pulses, R_s values remain above that of the reference. This is likely due to the formation of resistive silicides on top of SiC with still a rectifying interface in between. In this low ED regime, Raman spectra confirm the SiC decomposition onset, with the appearance of graphite related peaks (data not shown). Higher EDs promotes the local melt (then solidification) of circular areas. The de-wetting of these regions leads to craters (Fig.1b).

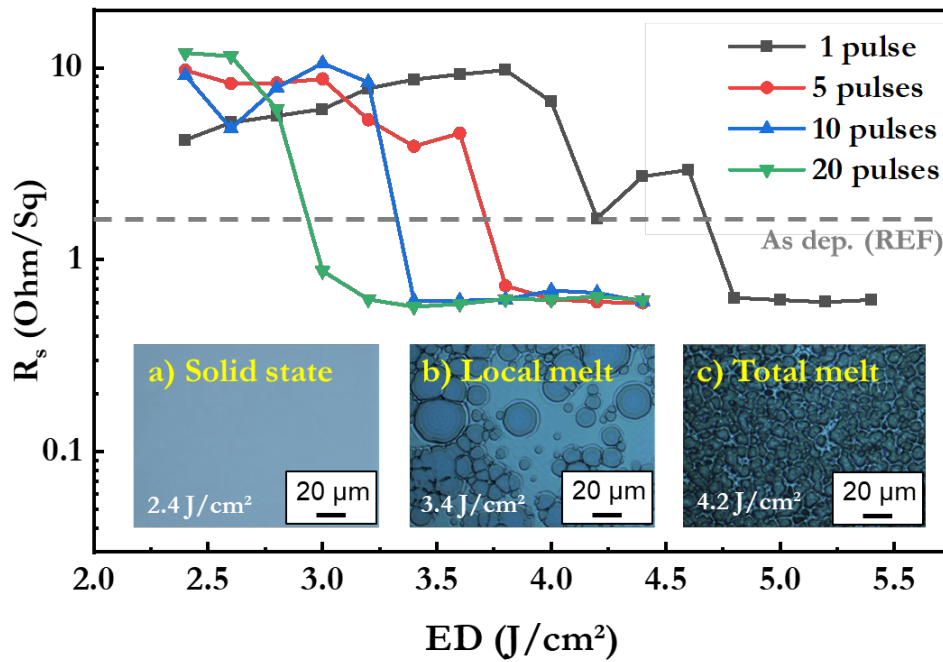


Fig. 1. Evolution of the sheet resistance after NLA on 80 nm Ni/4H-SiC stack as a function of pulse number and ED. Optical microscope observations for the 10 pulses series show the three main regimes, that is to say a) solid-state, b) local melt and c) total melt.

Raman spectra in those craters (Fig.2) reveal an interesting Silicon (Si) signature, likely associated with the formation of Si grains, as observed by Rascunà et al. [2] using STEM cross sections. The third regime, encountered for high ED, tallies with the complete top layer melt. Optical microscopy (Fig.1c) and SEM (Fig.5a) top views show a reacted layer (called core) with a protrusions network (called filaments) coming from de-wetting. Raman spectra acquired in core areas show well defined and intense Carbon (C) peaks, Si and SiC signals (Fig. 5e). In contrast, only C peaks are detected in filaments regions (Fig. 5e). In this regime, R_s drops below that of the reference, reaching a value corresponding to that of the 4H-SiC substrate, e.g. an interface losing its Schottky behavior. In addition, the R_s drop, the top layer melt onset, and the Si-rich silicide phases formation are shifted towards lower ED as the number of pulses increases.

When the wafer is processed at 400°C (heating chuck), these microstructural evolutions follow the same trend with another shift towards lower EDs. Thus, both the use of a heated chuck and several pulses at the same location enable a reduction of the required ED to get a specific microstructure. In the next part, these material features will be linked to ohmicity and resistance of the contacts.

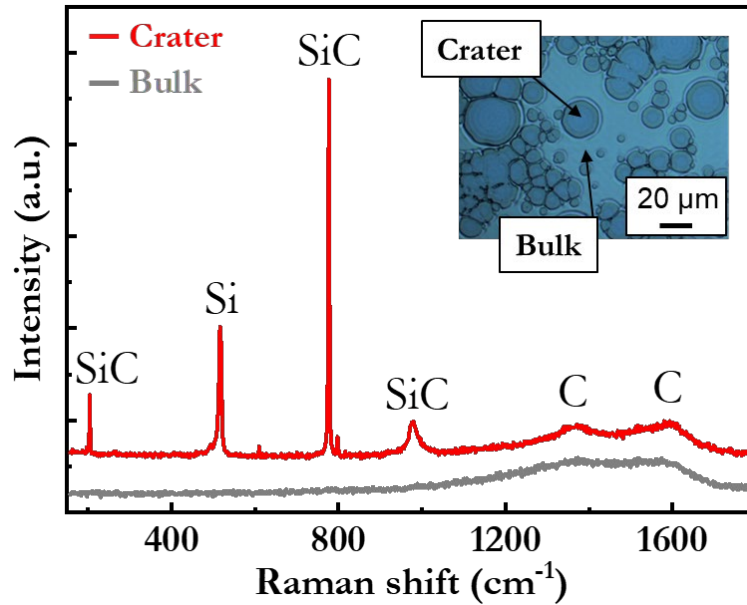


Fig. 2. Raman spectra after NLA on 80 nm Ni/4H-SiC, for 1 pulse at 4.4 J/cm² in bulk and crater regions (RT processing). For sake of clarity curves are shifted in intensity.

Contact resistivity & phase sequence. Fig.3 compares the contact resistivity as a function of ED for (i) the 1 pulse series at 400°C, (ii) the 10 pulses series at RT and (iii) the 10 pulses series at 400°C. First of all, a single pulse at RT was not sufficient to achieve ohmicity. On the contrary, some EDs lead to perfect linear I-V curves for the 10 pulses series at RT, with a minimum contact resistivity around $5 \times 10^{-5} \Omega \text{ cm}^2$ reached at 4.3-4.4 J/cm². Such a value is similar to that reported after RTP [4] and laser annealing [5] for the same SiC doping level. For the 10 pulses series at RT, the last comment pertains to the first ohmic condition ED, 3.6 J/cm², that is to say 0.2 J/cm² beyond the R_s drop. Thus, this R_s drop is a necessary condition but not sufficient. The use of the heating chuck, with then a 400°C process temperature, enables, for 1 or 10 pulses, to access ohmicity and even lower the contact resistance to $10^{-5} \Omega \text{ cm}^2$, e.g. a value significantly lower than those obtained with RTP [6], [7]. Therefore, ohmicity is found for the 1 pulse series at 400°C, with a significant productivity benefit compared to RT processing of N⁺ substrate (Fig.3).

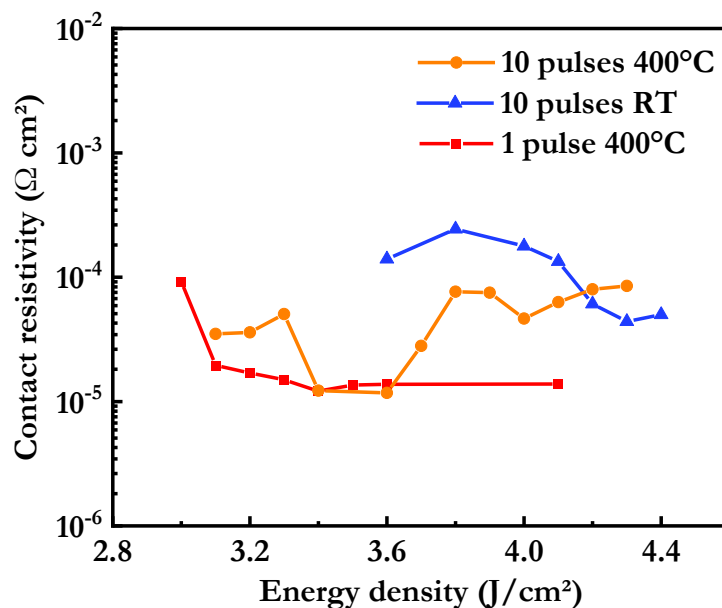


Fig. 3. Contact resistivity evolution after NLA on 80 nm Ni/4H-SiC stack, as a function of the applied ED for (i) the 1 pulse series at 400°C, (ii) the 10 pulses series at RT and (iii) the 10 pulses series at 400°C.

Raman spectroscopy, as a local and non-destructive method is used to investigate the formed silicides' nature. The phase sequence of the 10 pulses series at 400°C is shown in Fig.4. For low applied ED ($< 2 \text{ J/cm}^2$), a Ni_2Si phase is clearly evidenced. Then, at intermediate ED, the Ni-rich phase is replaced by NiSi . From 2.6 J/cm^2 and beyond, clear peaks are no more present. A possible explanation, drawn from the standard Ni-Si phase sequence [8], could be the formation of a Si-rich NiSi_2 phase, which is known to be barely active in Raman. Such a feature might explain the origin of ohmicity. Classical rapid thermal annealing used to form ohmic contacts usually promotes Ni_2Si formation. In NLA, ohmic contacts would rather be obtained when NiSi_2 is formed instead of Ni_2Si or NiSi . It supports the theory that mechanisms other than the presence of specific phases are the reason for ohmic contact formation. As proposed in the literature, carbon vacancies, formed during the silicidation process, may act as donors, resulting therefore in the formation of ohmic contacts [9]–[11]. Raman investigations, through C peaks analysis with ED, pulse number and chuck temperature, might help in understanding the role of released C.

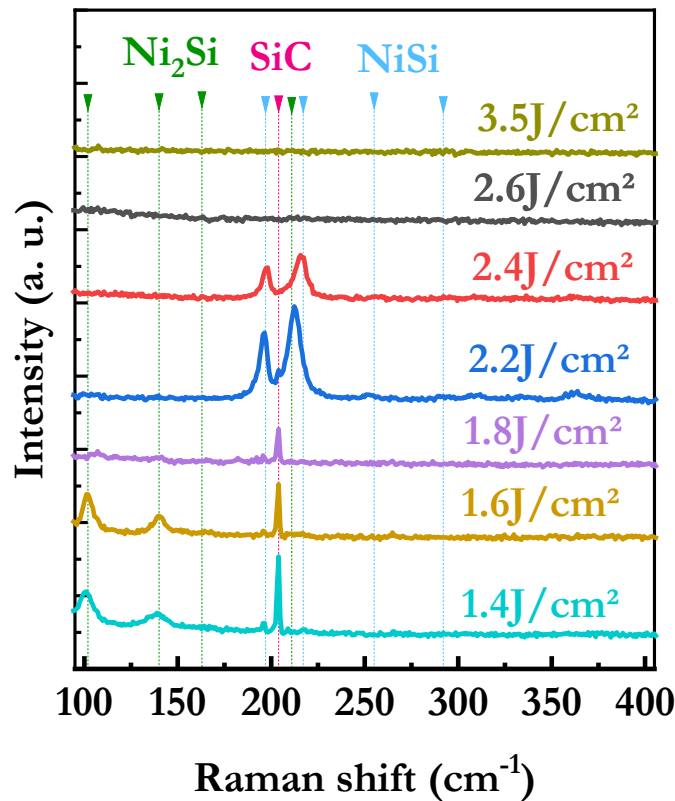


Fig. 4. Raman spectra after NLA on 80 nm Ni/4H-SiC, for the 10 pulses series processed at 400°C for ED between 1.4 to 3.5 J/cm^2 in core regions (for sake of clarity curves are shifted in intensity).

TEM observations. High-angle annular dark-field imaging (HAADF) STEM cross sectional images (Fig. 5b) of our electrically quasi-optimal sample at RT (4.4 J/cm^2 -10 pulses) confirm the bi-layer structure consisting in a reacted layer (Fig. 5c) with protrusions on top (Fig. 5d). Both regions contain C-clusters of different sizes distributed into a nickel silicide matrix. A quasi-continuous C-rich layer covers all areas. Between protrusions, the reacted layer clearly contains silicide crystalline grains and a relatively rough interface with SiC. Its thickness reaches roughly 200 nm, e.g. a value more than twice that the initial Ni layer. Filaments are 100 to 500 nm high. The interface below these regions seems smoother.

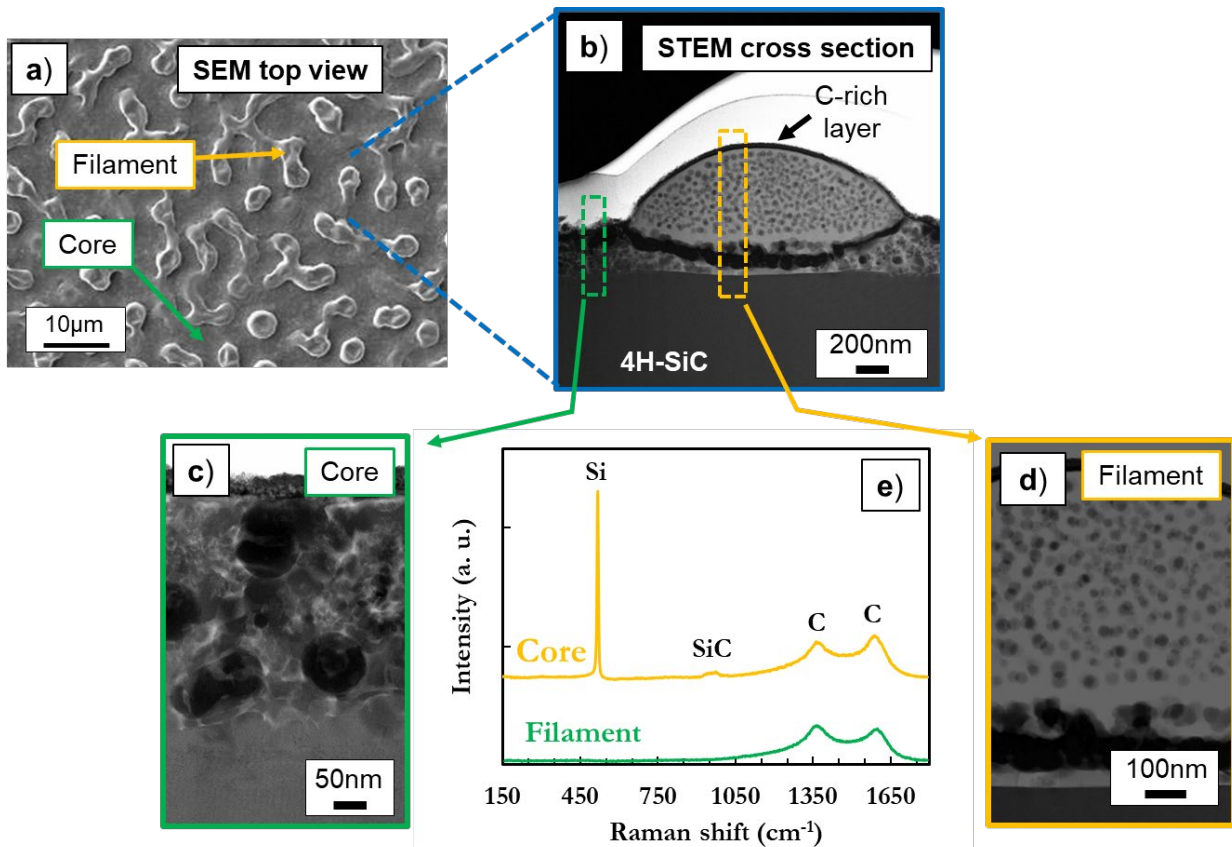


Fig. 5. a) SEM top view and b) STEM cross section image of the 4.4 J/cm²-10 pulses sample processed at RT, with HAADF-STEM observations in the c) core and d) filament areas. e) Associated Raman spectra showing Si, SiC and C peaks.

Conclusions & Perspectives

In conclusion, 80 nm Ni/4H-SiC samples were processed with NLA using single and multipulse approaches over a wide ED range. The influence of the chuck temperature was also investigated. Based on extensive material (OM, SEM, STEM, Raman) and electrical characterisations (sheet resistance / contact resistance), the following conclusions can be drawn:

- For all series, a common scenario is noticed when increasing ED, with first solid-state reactions, then some local melt and finally the complete top layer melt and de-wetting for high ED values. When the top layer continuously melts, the sheet resistance drops. This condition turned out to be necessary but not sufficient for contact ohmicity. Both multipulse and hot chuck enable to shift this R_s drop towards lower EDs and reduce therefore the thermal budget.
- When the 80 nm Ni/4H-SiC stack is processed at RT with a sufficiently high ED, the microstructure resulting from multipulse NLA (in terms of C redistribution and particular reacted layer / 4H-SiC interface) yields contacts with a specific resistivity at the state of the art.
- This is further improved using a 400°C heating chuck during the processing. In this case, a single pulse can yield ohmic contacts with a low thermal budget. A contact resistance as low as $10^{-5} \Omega \text{ cm}^2$ is then achieved for the investigated doping level of the SiC substrate.
- Last, Raman reveals key information on phase sequence, notably showing that the silicide phase is not the critical parameter for ohmicity.

The work could be extended in some parts. First, promising results obtained with the processing at 400°C have to be optimized. In addition, Ni thickness reduction and/surface preparation could possibly open new options for contact formation. Finally, the role of C-clusters has to be better understood.

References

- [1] P. Badalà *et al.*, « Ni/4H-SiC interaction and silicide formation under excimer laser annealing for ohmic contact », *Materialia*, vol. 9, p. 100528, 2020.
- [2] Rascuna et al., « Morphological and electrical properties of Nickel based Ohmic contacts formed by laser annealing process on n-type 4H-SiC », *Materials Science in Semiconductor Processing*, vol 97, p. 62-66, 2019.
- [3] F. Mazzamuto et al. , « Low Thermal Budget Ohmic Contact Formation by Laser Anneal », *Mater. Sci. Forum*, vol. 858, p. 565-568, 2016.
- [4] T. Kimoto et J. Cooper, *Fundamentals of Silicon Carbide Technology*, 2014, Singapore; Wiley.
- [5] Z. Zhou et al., « Characteristics of Ni-based ohmic contacts on n-type 4H-SiC using different annealing methods », *Nanotechnol. Precis. Eng.*, vol. 4, n° 1, p. 013006, 2021.
- [6] S. Liu et al., « A method to improve the specific contact resistance of 4H-SiC Ohmic contact through increasing the ratio of sp^2 -carbon », *Appl. Phys. Lett.*, vol. 117, n° 2, p. 023503, 2020.
- [7] F. La Via et al., « Schottky ohmic transition in nickel silicide 4h-SiC system Is it really a solved problem », *Microelectronic Engineering*, p. 519-523, 2003.
- [8] D. Mangelinck et al., « Mechanisms of Silicide Formation by Reactive Diffusion in Thin Films », *Diffus. Found.*, vol. 21, p. 1-28, 2019.
- [9] I. P. Nikitina et al., « Formation and role of graphite and nickel silicide in nickel based ohmic contacts to n-type silicon carbide », *J. Appl. Phys.*, vol. 97, n° 8, p. 083709, 2005.
- [10] S. Y. Han *et al.*, « Ohmic contact formation mechanism of Ni on n-type 4H-SiC », *Appl. Phys. Lett.*, vol 79, p.1816 (2001).
- [11] F. Roccaforte *et al.*, « Emerging trends in wide band gap semiconductors (SiC and GaN) technology for power devices », *Microelectron. Eng.*, vol. 187-188, p. 66-77, 2018.